STRUCTURAL AND FUNCTIONAL CHARACTERIZATION OF A LYMPHATIC SYSTEM USING COMPUTATIONAL AND EXPERIMENTAL APPROACHES

A Dissertation

by

ARUN MADABUSHI VENUGOPAL

Submitted to the Office of Graduate Studies of
Texas A&M University
in partial fulfillment of the requirements for the degree of

DOCTOR OF PHILOSOPHY

May 2008

Major Subject: Biomedical Sciences

STRUCTURAL AND FUNCTIONAL CHARACTERIZATION OF A LYMPHATIC SYSTEM USING COMPUTATIONAL AND EXPERIMENTAL APPROACHES

A Dissertation

by

ARUN MADABUSHI VENUGOPAL

Submitted to the Office of Graduate Studies of
Texas A&M University
in partial fulfillment of the requirements for the degree of

DOCTOR OF PHILOSOPHY

Approved by:

Chair of Committee,	Randolph H. Stewart
Committee Members,	Christopher M. Quick
	Glen A. Laine
	David C. Zawieja
Head of Department,	Glen A. Laine

May 2008

Major Subject: Biomedical Sciences

ABSTRACT

Structural and Functional Characterization of a Lymphatic System Using Computational and Experimental Approaches.

(May 2008)

Arun Madabushi Venugopal, B.E., University of Madras;

M.S., Texas A&M University

Chair of Advisory Committee: Dr. Randolph H. Stewart

The lymphatic system returns interstitial fluid back to the blood circulation. They have a network of vessels with numerous lymphangions, the segment of lymphatic vessel between two unidirectional valves. The valves aid in transporting lymph against a pressure gradient, in addition to the lymphangion pump which exhibit cyclical variations in diameter. Like blood vessels, baseline lymphatic tone is regulated with changes in transmural pressure; however, the transient response of lymphatic diastolic diameter following changes in transmural pressure has not been studied. The lymphangion pump is often described using cardiac analogies. However, since an active system empties into another active system in a lymphatic vessel, the analogy cannot characterize the principles governing optimal lymphatic vessel function. Furthermore, to optimize lymph flow there is also a need to characterize the lymphatic network structure.

To characterize the transient diameter response of lymphatic segment, we used post-nodal bovine mesenteric lymphangions in an isobaric preparation and measured the

diameter response to a step change in pressure. An immediate active reduction in end-diastolic diameter with each incremental increase in pressure was observed.

To identify the principles governing optimal lymphatic vessel function, we applied the result obtained from optimizing the interaction of the heart-arterial system to measured lymphangion pressure-volume relationships. We assumed that the slope of end systolic pressure-volume relationship (E_{max}) is equal to the slope of end-diastolic relationship (E_{min}) above a cutoff pressure and $E_{max}>E_{min}$ below the cutoff pressure. Unlike the heart, we found that stroke work is not optimized when $E_{max} = E_{min}$. However, there is a region where lymph flow is insensitive to changes in transmural pressure.

To characterize the lymphatic network structure, we used an approximation of time-varying elastance model. We found there is an optimal length for the lymphangion when it produces maximal flow. To develop a fractal network model, we determined the ratio of radius and ratio of length of lymphangion at a confluence. Using conservation of mass and certain simplifying assumptions, we showed that the ratio of radius, as well as ratio of length of upstream lymphangion, to the downstream lymphangion at confluences is 1.26.

To my parents

ACKNOWLEDGEMENTS

I would like to thank my advisor Dr. Randolph Stewart for his guidance, patience, and invaluable advice through out the course of my research. I would also like to thank Dr. Christopher Quick, who believed in my capabilities, and gave me a chance to take up research. Both of them have been instrumental in developing my skills to perform experiments and develop mathematical models.

I would also like to thank Dr. Glen Laine for providing guidance as my committee member, and also for the insights he has provided during various stages of my dissertation.

My fellow graduate students, Ketaki Desai, Waqar Mohiuddin, Ranjeet Dongaonkar, Jay Widmer, Phuc Nguyen and Josh Meisner have been helpful in providing valuable comments and criticism, and I thank them for their support overall. I would especially like to thank Ketaki, for being a good friend and a colleague, without whom a lot of late-nights would not have been possible.

I would also like to thank my friends Vikram, Nikhil, Vijay, Preethi, Indira, Arjun, Parikshith, Sarath, Deepak, Anusha and many others for making my life in College Station enjoyable.

Most of all, I would like to thank my family for their endless support and motivation. My brothers Arvind and Arjun and my sister-in-law, Neha have provided me with their love and support. I specially thank my parents who have always provided me with the best of everything.

TABLE OF CONTENTS

LIST OF FIGURES

FIGURE Page

FIGURE Page

1. INTRODUCTION

1.1 OVERVIEW

Lymphatic vessels ensure lymph flow under varying conditions. One of the primary purposes of the lymphatic system is to return fluid from the lower-pressured interstitial space to the higher-pressured veins (57). Lymphangions, the fundamental functional unit of the lymphatic system, consists of a section of lymphatic vessel bounded by two unidirectional valves (39). Lymphangions contract cyclically and actively pump lymph, inviting analogies to contracting cardiac ventricles and useful characterizations such as systolic and diastolic periods (4), stroke volume (15, 34), and even stroke work (34). The lymphangion pump has to adapt to keep interstitial pressure (and thus interstitial volume) low on the one hand (4) and to maintain lymph flow when faced with venous hypertension on the other. Although these functional challenges may be met by altering pump behavior in response to flow (23, 45), they are primarily met by responding to changes in pressure (37). Failure of lymphangions to functionally adapt can exacerbate interstitial edema, the accumulation of excess fluid in the interstitial space. Different edemagenic stresses, however, can result in different lymphangion transmural pressures. For instance, with an increase in microvascular pressure, microvascular filtration, and thus lymphangion transmural pressures, can increase up to 5 mmHg (4). With venous hypertension, lymphatic outlet pressure and, thus, lymphangion pressures can presumably increase as high as central venous pressure (11).

This dissertation follows the style of *American Journal of Physiology.*

Lymphatic vessel response to pressure and flow. Lymphatic vessel contractions are modulated by hydrostatic pressure and lymph flow within the vessel, the two main functional variables. Lymphatic vessels respond to increased transmural pressure with increases in stroke volume and contraction frequency (37). Stroke volume exhibits a peak at a transmural pressure of approximately 5 cmH_2O and declines at higher pressures (17, 37). Flow acts to inhibit contractility (23). Separating the effects of flow from those of pressure, Gashev et al. demonstrated that flow-induced inhibition of lymphatic pump activity in isolated rat mesenteric lymphatics and thoracic duct exhibited two stages (23). First, contraction frequency was rapidly inhibited, an effect that decreased with time of exposure to increased flow. Second, a sustained inhibition of the amplitude of contraction developed with continued exposure to increased flow. Second, a sustained inhibition of the amplitude of contraction developed with continued exposure to increased flow. This latter behavior is similar to that exhibited by arterioles, where endothelial shear stress induces release of nitric oxide from the endothelium, resulting in smooth muscle relaxation (31).

Diameter response of arterioles and venules to step changes in pressure. Arterioles respond to an elevation in transmural pressure with constriction and to a pressure reduction with dilation (6). This property of arterioles was originally termed the "myogenic response" by Bayliss et al. in 1902 (2). A similar response has been identified in venules. Venules in the bat wing in particular exhibit spontaneous venomotion, and respond to changes in pressure by increasing both frequency and amplitude of venular contraction (7). In both arterioles and venules, with an increase in

pressure, an immediate increase in end-diastolic diameter is followed by a transient active reduction of the diameter. Likewise, a decrease in pressure induces an immediate decrease in end-diastolic diameter followed by a transient dilation. At steady-state, however, venular end-diastolic diameter increases with increasing pressure.

Steady state-lymphatic myogenic response. Mizuno et al. (40) and Hosaka et al. (28) reported that the steady-state end-diastolic diameter of rat iliac lymphatic vessels did not change significantly in response to increases in transmural pressure. However, there was an increase in end-systolic diameter with an increase in pressure, thus reducing the amplitude of contractions. The transient diameter change of lymphatic vessels in response to altered pressure, however, has not been previously reported.

Lymphangion mathematical models based on analogies to cardiac ventricles and blood vessels have played critical roles when experimental approaches were intractable. Reddy et al. were the first to develop a model of an entire lymphatic system based on the Navier-Stokes equations, classically used to predict the flow through blood vessels from fundamental physical principles (47). The resulting model determined how lymph viscosity, inertia, and cyclical contraction affect pressures and flows throughout the entire lymphatic system (48), which are not feasible to measure experimentally. In a distinctly different approach, Quick et al. developed a model to describe lymphatic function based on the time-varying elastance concept (i.e., the ratio of transmural pressure and volume) (46), classically used to characterize cardiac ventricles (50, 51). Since the model selectively simplified complex phenomena, the resulting algebraic formula provided the critical insight that the “effective resistance” of a lymphatic system

actually is a function of lymphangion contractility and contraction frequency (46). In a hybrid approach, Quick et al. combined a model of blood vessels based on the classical transmission-line description and a model of the ventricle based on time-varying elastance (45). The model, developed from measured lymphangion properties, correctly predicted that lymphangions transition from active pumps to passive conduits when inlet pressure rises above outlet pressure. This lymphangion model was extended by Venugopal et al. to demonstrate that coordination of contraction between adjacent lymphangions (which cannot be controlled experimentally) has minimal effect on lymph flow (55). Taken together, these approaches illustrate the advantages of mathematical models when they are 1) based on measured lymphangion properties, 2) incorporate fundamental physical properties, and 3) selectively simplify complex phenomena.

Lymphangions are notably different than ventricles or blood vessels. Although critical for developing mathematical models of lymphatic vessels, analogies to blood vessels and cardiac ventricles do not completely capture lymphatic vessel behavior. For instance, comparing a large-scale, complex model of a lymphatic vessel (based on blood vessel properties) (55) with a simple algebraic approximation revealed that lymph viscosity and inertia have negligible effects on lymph flow in post-nodal vessels (46). Models incorporating lymph viscosity and inertia to predict lymph flow are therefore needlessly complex. Furthermore, the lymphatic mathematical model developed by Drake et al. (15) assumed pressure-volume relationships with relatively linear end-diastolic pressure-volume relationships. Unlike the ventricle, however, the lymphangion end-diastolic pressure-volume relationship is highly nonlinear (4, 34, 43) and results

from an active tone (28). Finally, heart-arterial system coupling results from an active pump emptying into a passive arterial network. This is qualitatively different from lymphangion-lymphangion interaction arising from two active pumps (36, 55, 58). The theoretical differences in the description of lymphangions and cardiac ventricles in particular must be addressed to fully exploit these extensive tools to model lymphangion-lymphangion interaction.

Principles governing arterial network structure. The principles governing lymphatic network structure have not been well characterized, in contrast to the advances made in identifying the principles governing the structure of the arterial system (42). Although transporting blood from the heart to the capillaries requires numerous bifurcations to achieve a 3-order of magnitude reduction in arterial diameter, most of the radii of an arterial tree can be predicted using Murray's Law (42). Using analytical methods and mathematically minimizing energy loss at a bifurcation results in a prediction that the cube of a mother vessel radius is equal to the sum of the cube of its daughter vessels. To arrive at this prediction, it was assumed that mean blood flow is governed by Poiseuille's Law and conservation of mass governs flow through the bifurcations. This theoretical prediction was subsequently validated by a number of experimental studies (49, 54). Despite important criticism (44), the finding that arteries adapt to maintain shear stress within a relatively narrow (10-100 dynes/cm^2) range (30) eventually provided the missing mechanism giving rise to this theoretical branching rule. The success of Murray's Law to predict the structure of an entire arterial network has however yet to be replicated for the lymphatic system.

Optimality principles suggested from heart-arterial system interaction. Although the physics governing lymph flow (45, 55) and lymphangion mechanics (47, 59) are well understood, the principles governing lymphangion-lymphangion coupling have just beginning to be studied (55). Insight may be gained by exploring the principles governing optimal heart-arterial interaction, postulated by Sunagawa et al (52). Because it is not possible to alter heart and arterial system experimentally over wide ranges, they derived a simple algebraic formula for estimating the stroke volume as a function of the slope of the end-systolic pressure-volume relationship (E'_{max}) and the "effective arterial system elastance" (E'_a). Stroke work was found to be optimized (maximized) when $E'_{max}=E'_a$. Although lymphangions actively pump like the heart, each lymphangion empties into another actively pumping lymphangion. Thus, the cardiac analogy to define an optimal coupling of lymphangions may not hold.

Use of mathematical models to reveal optimality principles. *Use of mathematical models to reveal optimality principles*. Whenever there is a cause and effect relationship between two different variables, there can be a case made for the dependent variable to have an optimum. One such relationship was experimentally demonstrated for the stroke work of lymphangion which had an optimum at a particular distending pressure (1). However, this was a purely functional study, allowing us to draw minimal conclusions about the relationship between the lymphangion structure and stroke work. Relating structure to function is typically challenging, since the structural parameters cannot be made an experimental variable. This can, however, be achieved using mathematical modeling, which allows us to use treat fixed parameters like those describing structure as

variables. Although these models were evaluated numerically, they allowed manipulation of parameters such as length and contractility that cannot be experimentally controlled (56). The complexity of numerical solutions, however, increases dramatically when attempting to model more than a few lymphangions, because of the large number of required parameters. This was true of the model developed by Reddy et al., who attempted to model the larger vessels of an entire lymphatic network (48). One of the critical limitations of detailed large-scale modeling approach is that its complexity is not amenable to the discovery of fundamental optimality principles like Murray's Law. In order to reduce the complexity inherent in numerically-evaluated models, Quick et al. (46) developed an analytical (i.e., algebraic) equation to describe the lymphangion pressure-flow relationship (10, 13). Analytical equations are also useful in describing a network of vessels, similar to the fractal models used to describe the microcirculation (26). These fractal models are based on simple branching rules which ultimately predict the structure of the entire tree. Murray's Law uses one such analytical equation to describe the tree of blood vessels. The analytical model developed previously can thus be useful in predicting the fractal structure of the lymphatic vessel along with the flexibility it provides in predicting an optimal lymphatic tree.

Thus, the purpose of the present work is to

1. Characterize the transient response of lymphatic vessels to changes in transmural pressure.

2. Use mathematical modeling to determine the ideal lymphangion properties that optimize lymphatic vessel function.
3. Determine the structure of a lymphatic network that optimizes lymph flow.

2. LYMPHATIC MYOGENIC RESPONSE

2.1 METHODS

Experimental preparation. Post-nodal bovine mesenteric lymphatic vessels were obtained from an abattoir immediately after slaughter. Following careful removal of fat and connective tissue, the vessels were transported to the laboratory at approximately 30°C in 1% albumin physiological saline solution (APSS) containing, in mM, 145 NaCl, 4.70 KCl, 2.00 $CaCl_2$, 1.17 $MgSO_4$, 1.20 NaH_2PO_4, 5.00 dextrose, 2.00 sodium pyruvate, 0.020 EDTA, 3.00 MOPS buffer and 10g/L of albumin. Valveless lymphatic segments were resected and cannulated in a tubular organ bath (Fig. 2.1). The bath and lumen of the vessel were perfused with APSS at 37°C with a pH of 7.4, with no transmural oncotic pressure differential. Flow through the bath was set to 25% of the bath volume per minute. The bath and luminal solutions were gassed with room air using a membrane oxygenator (OXR, Living Systems Instrumentation, Burlington, VT).

Data acquisition. Images of the lymphatic segment were acquired by a monochrome camera (ST-XC50, Sony Electronics, Park Ridge, NJ) and captured by a video card (IMAQ, National Instruments, Austin, TX). External diameter was measured using a custom-designed program (LabVIEW, National Instruments, Austin, TX) that identified the outside edges of the vessel wall. Luminal pressure (P_l) was measured at the inlet end of the vessel with a pressure transducer (PX26-001GV, Omega, Stamford, CT), and the transmural pressure (P_t) of the vessel was calculated,

$$P_t = P_l - P_e \tag{2.1}$$

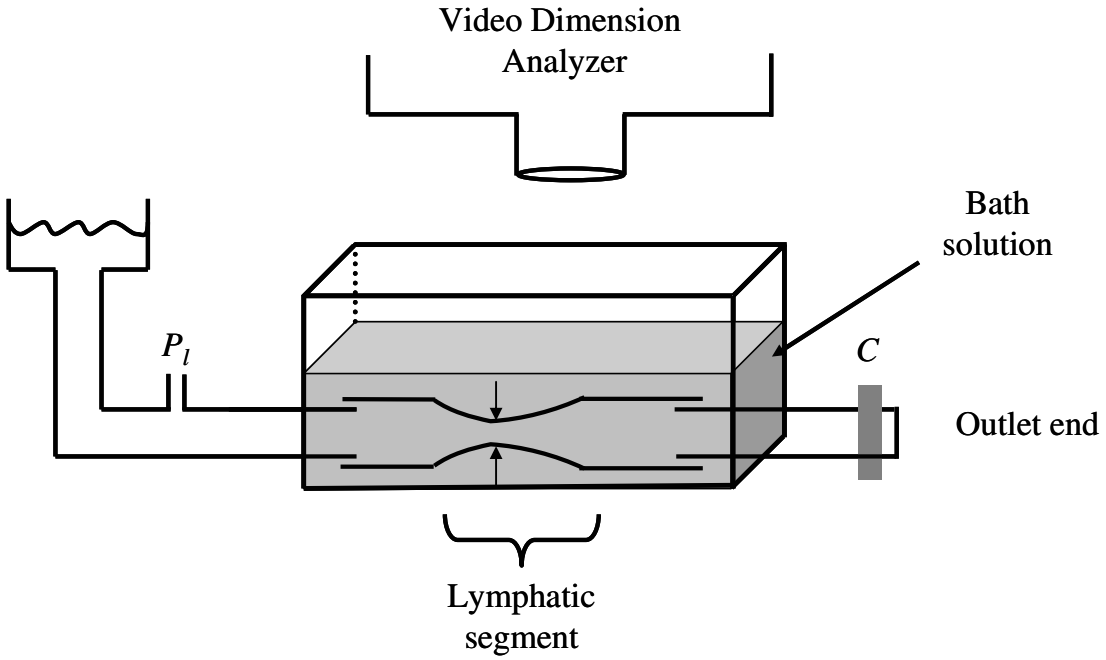

Figure 2.1: Experimental apparatus. This schematic demonstrates experimental preparation of a lymphatic segment submerged in a polyionic bath solution, designed to measure pressure (P_l) at the inlet end and diameter using a video dimension analyzer for an isobaric preparation with the outlet end blocked using a clamp (C).

where P_e is the external pressure determined from depth of the vessel in the bath solution. The measured diameter and luminal pressure were then acquired (DAQ, AD Instruments, Colorado Springs, CO).

Isobaric conditions. To evaluate the effect of transmural pressure on lymphatic vessel contraction, lymphatic segments were subjected to isobaric conditions, i.e., the transmural pressure was maintained near constant during each measurement period. The clamp at the outlet end (Fig. 2.1) was closed to minimize endothelial shear stress; however, shear stress was not completely eliminated since fluid moved into and out of the vessel through the inlet port during the contraction cycle. Luminal and, thus, transmural pressures were adjusted by changing the height of the inlet cannula.

Experimental protocol. Baseline conditions for lymphangion contraction were established by allowing the lymphatic segment to contract at a transmural pressure of 3 mmHg for a minimum of 15 minutes. Only spontaneously contracting lymphatic segments which displayed periodic contraction during the equilibration period were used. The diameter and pressure were recorded throughout the experiments at a rate of 25 samples per second. In each experiment, the transmural pressure was increased from a baseline of 3 mmHg in four different pressure steps to approximately 6, 9, 12, and 15 mmHg. Lymphatic segments were maintained at each pressure step for a minimum of 5 minutes. This time period was established from the results of preliminary studies indicating that it was the time required for the transient response to be complete. After each pressure increase, the transmural pressure was returned to a baseline of 3 mmHg.

Data analysis. With a step change in pressure, data collected during three to five contraction cycles were averaged at three different time periods (Fig. 2.2): 1) PRE: immediately before the step change in pressure, 2) POST: immediately after the step change in pressure and 3) POST+4: four minutes after the step change in pressure. End-diastolic diameter, end-systolic diameter, stroke volume, and contraction frequency were calculated from the recorded diameter trace. Percent change in end-diastolic diameter, contraction frequency, and stroke volume were calculated for three comparisons: 1) PRE to POST, 2) POST to POST+4 and 3) PRE to POST+4. The stroke volume was calculated assuming a cylindrical structure, and was normalized by lymphangion length. The percent change in each variable was plotted as a function of the change in transmural pressure. These data were analyzed by linear regression. A result was considered to be statistically significant at $p \leq 0.05$.

2.2 RESULTS

Lymphatic myogenic response. Five lymphatic segments ranging between 2.4-6.0 mm external diameters (at end-diastole) were successfully instrumented. Figure 2.2 illustrates the effect of a step change in transmural pressure on end-diastolic diameter in a representative vessel. Briefly, a step increase in transmural pressure resulted in an immediate increase in end-diastolic diameter followed by a gradual decrease that reached steady-state in approximately 4 minutes. Conversely, a step decrease in pressure resulted in an immediate decrease in end-diastolic diameter followed by a gradual increase that reached steady-state in approximately 4 minutes.

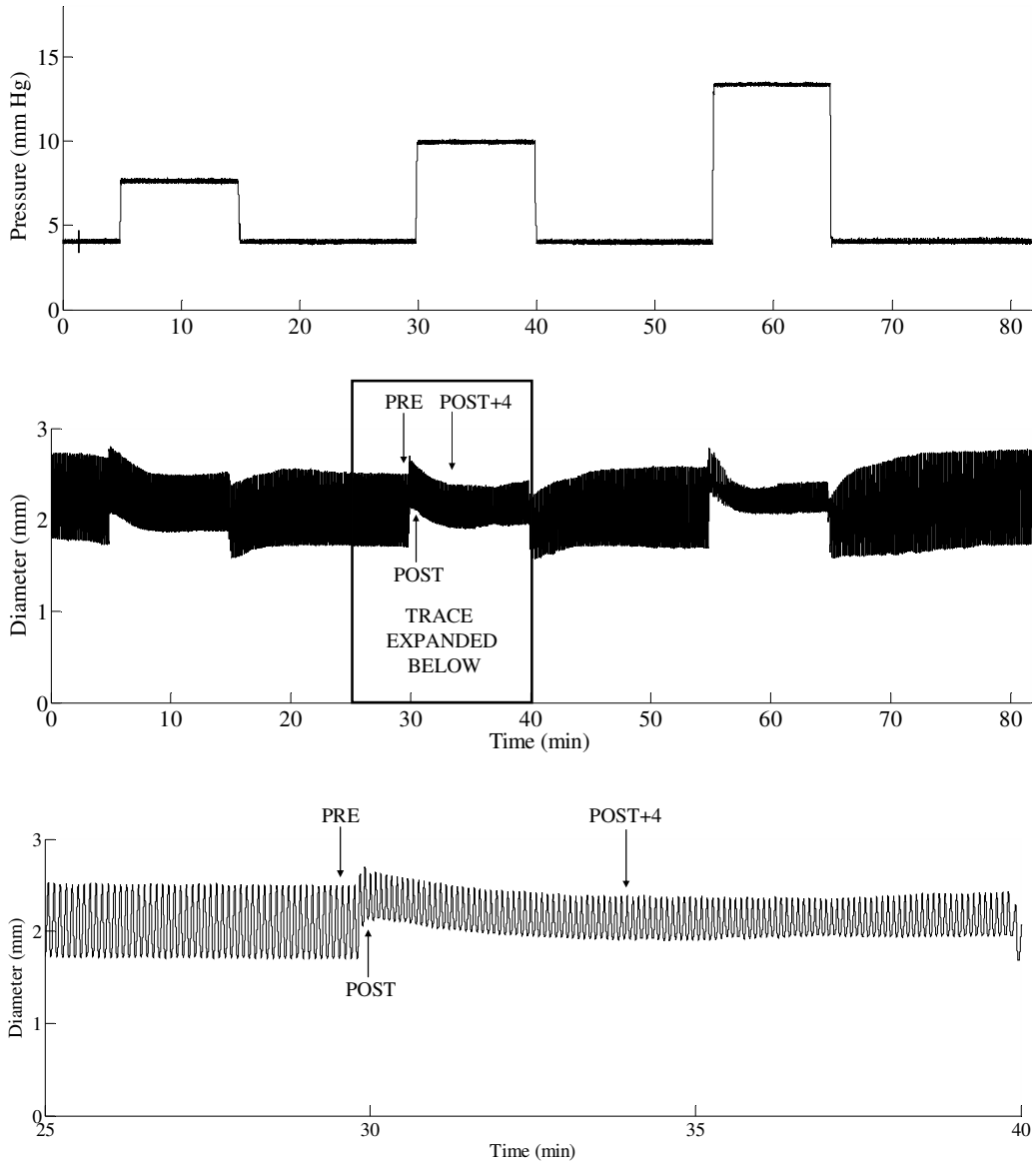

Figure 2.2: A representative tracing of the instantaneous lymphangion diameter response to step increases and decreases in transmural pressure. The bottom panel represents a close up of the diameter response. Contraction cycles were averaged at three different time periods: 1) PRE: immediately before the step change in pressure 2) POST: immediately after the step change in pressure and 3) POST+4: four minutes after the step change in pressure. The lymphatic myogenic response is complete within four minutes following the step change in pressure.

Lymphatic diameter response to a step change in pressure. Pooled diameter data indicate that the percent change in end-diastolic diameter from PRE to POST (Fig. 2.3A) was significant and positively related with the change in pressure. The percentage change from POST to POST+4 (Fig. 2.3B), i.e. the myogenic response, was also significant but was negatively related to the pressure change. This response was of sufficient magnitude that an increase in transmural pressure resulted in a net decrease in end-diastolic diameter from PRE to POST+4 (Fig. 2.3C). A regression of end-diastolic diameter at steady state and transmural pressure showed significant negative relationship.

Lymphatic frequency response to a step change in pressure. Regression of the percent change in lymphatic contraction frequency as a function of the step change in transmural pressure did not result in a slope significantly different from zero for any time comparison: PRE to POST, POST to POST+4 or PRE to POST+4 (Fig. 2.4).

Normalized lymphatic stroke volume with step changes in pressure. A significant negative relationship was detected between stroke volume and pressure change from PRE to POST (Fig. 2.5A). Stroke volume did not change significantly from POST to POST+4 (Fig. 2.5B). A significant negative relationship was detected between stroke volume and transmural pressure change from PRE to POST+4 (Fig. 2.5C).

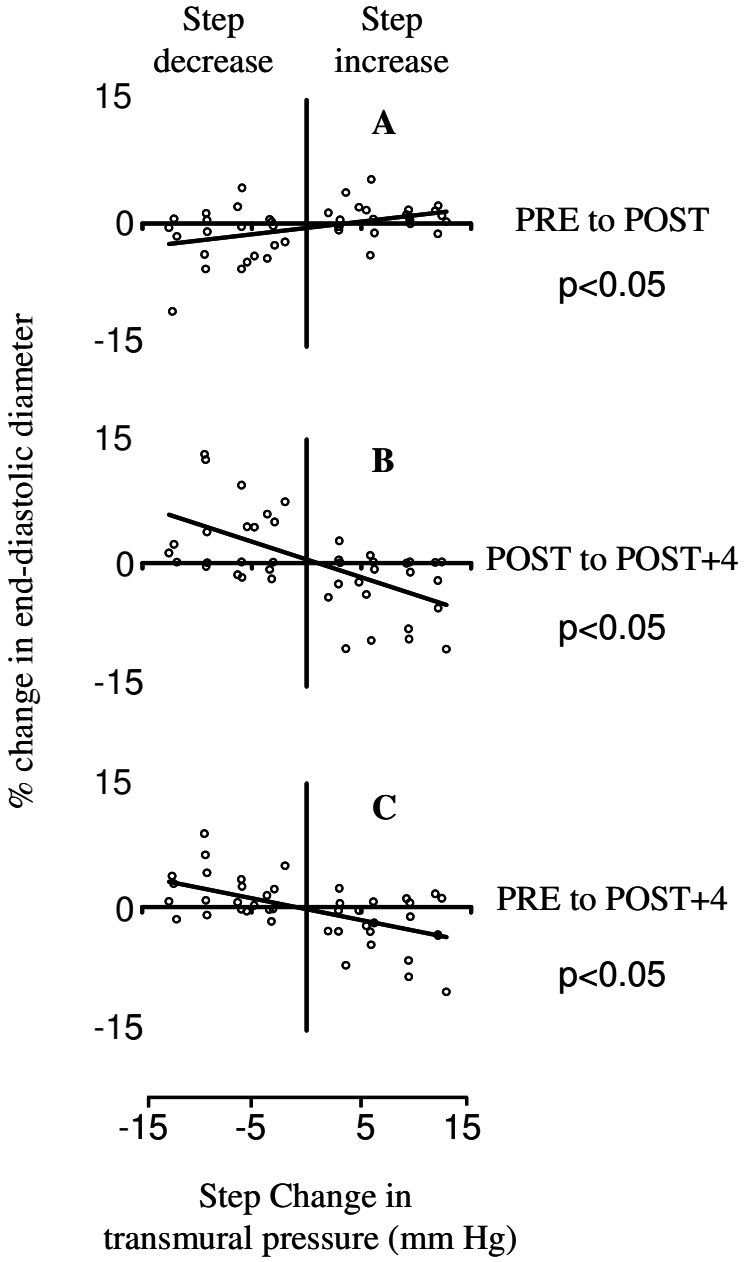

Figure 2.3: Effect of step change in transmural pressure to percent change in end-diastolic diameter. The percent change in end-diastolic diameter comparing A) PRE to POST, B) POST to POST+4, C) PRE to POST+4 (see Fig.2), had significant slopes of 0.15, -0.43,-0.27 respectively. There is a larger myogenic response with higher step changes in pressure.

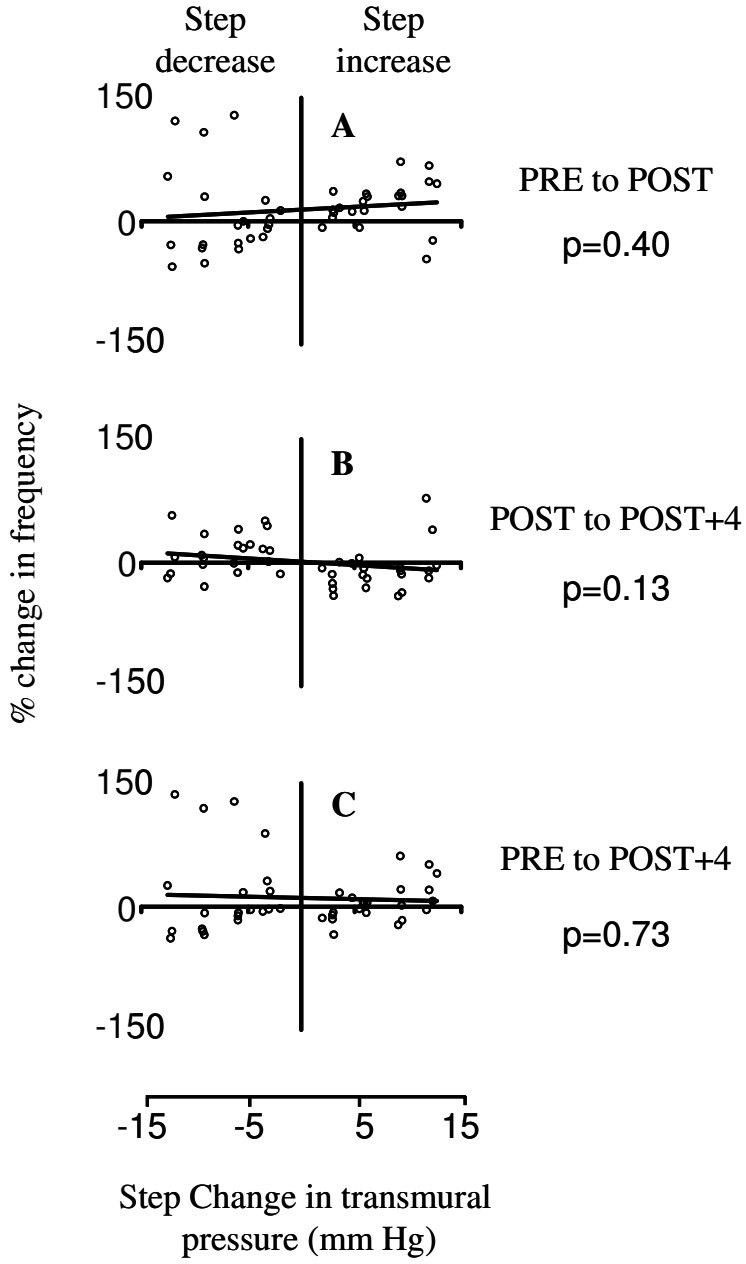

Figure 2.4 Effect of step change in transmural pressure to percent change in lymphatic contraction frequency. The percent change in lymphatic contraction frequency for A) PRE to POST, B) POST to POST+4, C) PRE to POST+4 (see Fig. 2.2), had slopes of 0.71 , -0.80 and -0.28 respectively with none of them having a slope significantly different than zero.

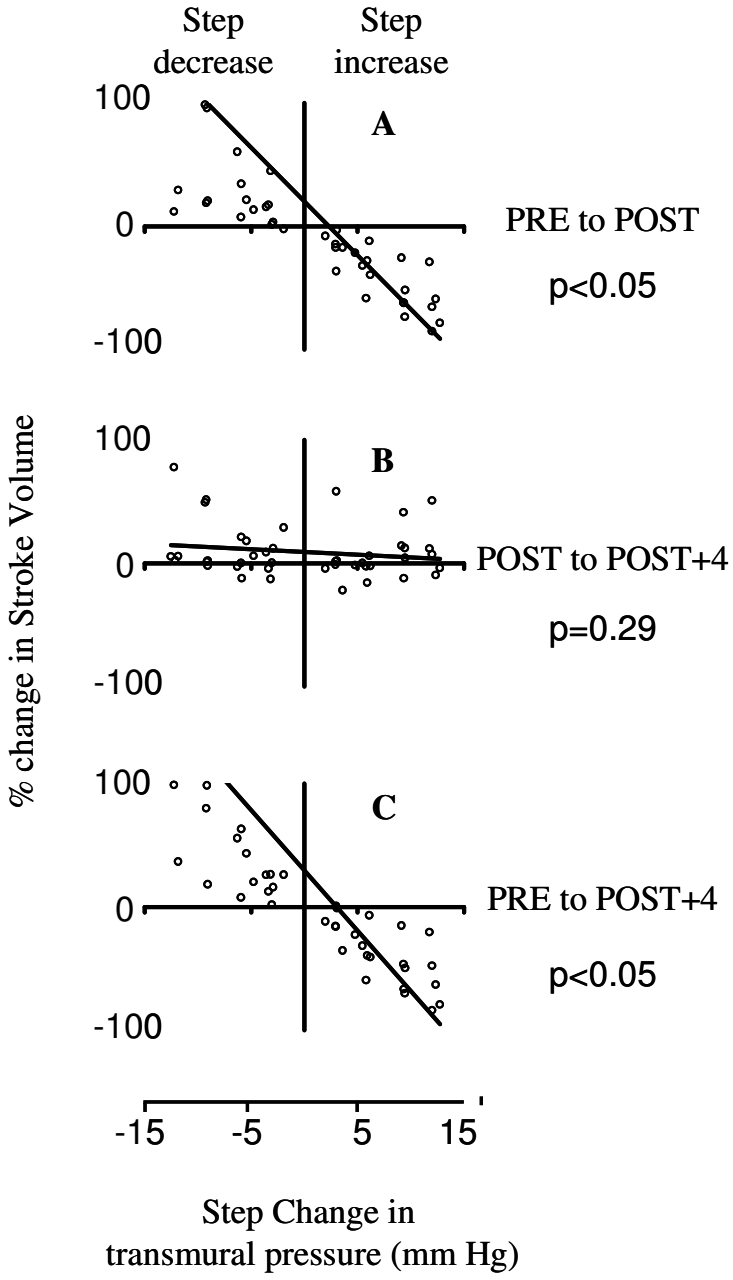

Figure 2.5: Effect of step change in transmural pressure to percent change in stroke volume. We were unable to demonstrate a significant stroke volume change for POST to POST+4 with a slope of -0.437, suggesting equal decreases in both end-systolic and end-diastolic diameter. The PRE to POST AND PRE to POST+4 (see Fig. 2.2), and had negative correlations with significant slopes of -8.7 and -9.8 respectively.

3. OPTIMAL LYMPHANGION PRESSURE-VOLUME RELATIONSHIP

3.1 METHODS

Analytical solution to describe lymphangion flow. Following the approach used to describe ventricular function (52), the stroke volume (*SV*) of a lymphangion was approximated (46), assuming that the pressure-volume loops are rectangular,

$$SV = \left(\frac{P_{in}}{E_{min}} - \frac{P_{out}}{E_{max}} + V_{o,ed} - V_{o,es} \right), \tag{3.1}$$

where P_{in} and P_{out} are the lymphangion inlet and outlet pressures, E_{min} and $V_{o,ed}$ are the slope and intercept of the end-diastolic pressure-volume relationship, and E_{max} and $V_{o,es}$ are the slope and intercept of the end-systolic pressure-volume relationship. By multiplying *Eq. 3.1* by the contraction frequency, lymphangion flow can be approximated. *Equation 1* was rigorously validated by comparing its predictions to a highly detailed, complex, realistic mathematical model (45, 55) and to experimentally measured lymph flow (46). The simple analytical solution (i.e., algebraic formula) expressed by *Eq. 3.1* not only provides insight into the relationship of lymphangion structure and function, but also provides the necessary basis to predict optimality principles.

Stroke work of a lymphangion. The lymphangion stroke work (i.e., external work done to lymph) can be calculated as the product of change in pressure (P_{in}-P_{out}) and *SV*,

$$SW = \left(P_{in} - P_{out}\right) \cdot SV \ . \tag{3.2}$$

The lymphangion pressure-volume relationship exhibits two zones of pressure. The time-varying elastance model used in earlier lymphangion models (45, 55) assumed a linear end-diastolic pressure-volume relationship. The lymphangion end-diastolic pressure-volume relationship, however, is a highly nonlinear function (34, 43). To represent the end-diastolic volume (V_{ed}) more accurately, we divided the end-diastolic pressure-volume relationship into two segments having different slopes based on transmural pressure (P_{tran}) values being below and above a cutoff pressure (P_c).

$$V_{ed} = \begin{cases} V_{o,ed1} + \dfrac{1}{E_{min1}} P_{tran}, P_t < P_c \\ V_{o,ed2} + \dfrac{1}{E_{min2}} P_{tran}, P_t > P_c \end{cases} \tag{3.3}$$

In this case, E_{min1} and $V_{o,ed1}$ is the slope and intercept of the end-diastolic pressure-volume relationship in the low-pressure zone (i.e., *Zone 1*), and E_{min2} and $V_{o,ed2}$ is the slope and intercept of the end-diastolic pressure-volume relationship in the high-pressure zone (i.e., *Zone 2*).

Deriving realistic parameters from bovine mesenteric lymphangions. Figure 1 illustrates an example of a bovine mesenteric lymphangion pressure-volume relationship, previously reported by Ohhashi et al. (43), which shares critical similarities with other reported pressure-volume relationships (4, 34). Data was digitized and imported into MatLab (The MathWorks Inc., Natick, MA). Linear regression of the end-systolic pressure-volume relationship yielded values for E_{max} $V_{o,es}$ and $V_{o,ed1}$. The value of E_{min2} (*Eq. 3.3*) was assumed equal to E_{max}, and nonlinear parameter estimation was used to estimate the value for P_c, E_{min1} and $V_{o,ed2}$ (minimizing least-squared error) (3).

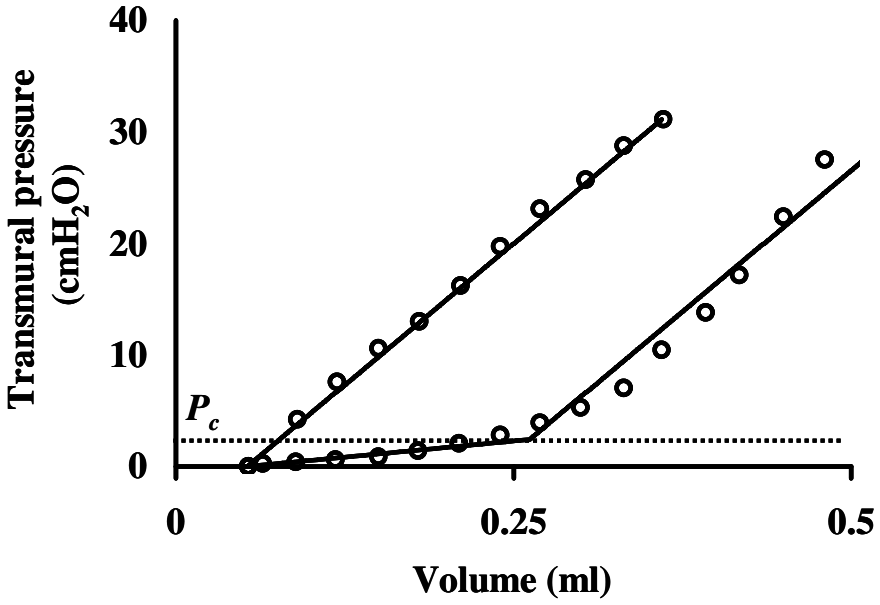

Figure 3.1: Pressure-volume relationship of a bovine mesenteric lymphangion digitized from Ohhashi et al. (43), (circles). Solid lines indicate approximate end-systolic pressure-volume relationship (ESPVR) and end-diastolic pressure-volume relationship (*Eq. 3.3*). Cutoff pressure (P_c) was identified using non-linear parameter estimation and slope of EDPVR was set to the slope of ESPVR above the cutoff pressure (E_{max}=E_{min}).

Stroke volume and stroke work for the two pressure zones. Stroke volume and stroke work were calculated for the two zones of pressure above and below P_c, (*Eq. 3.3*). In pressure *Zone 1*, E_{min1} was assumed to equal the value of E_{min1} derived from the data illustrated in Fig. 3.1. In pressure *Zone 2*, E_{min2} was assumed to equal E_{max}. Inlet pressure and outlet pressure were set assuming a differential pressure of 0.2 cmH_2O. The resulting stroke volume and stroke work were calculated from *Eqs. 3.1-3.3* and plotted as a function of transmural pressure.

Lymphangion-lymphangion coupling. To determine the stroke work of a lymphangion in a lymphatic vessel, we applied the principles developed by Sunagawa et al. (52) for heart- arterial system interaction. For simplicity of derivation, a lymphatic vessel with two lymphangions was assumed, although the results are independent of the number of lymphangions. It was assumed that the upstream lymphangion and the downstream lymphangion had the same stroke volume, $V_{o,es,}$ $V_{o,ed}$, E_{max} *and* E_{min}. The outlet pressure of the upstream lymphangion (P_t) is assumed equal to the inlet pressure for the downstream lymphangion when the upstream lymphangion is in systole and downstream lymphangion is in diastole. Solving for P_t in *Eq. 3.1* as a function of E_{max}, $V_{o,es}$ and V_{ed},

$$P_t = E_{max}\left(\frac{P_{in}}{E_{min}} - SV - V_{o,es} + V_{o,ed}\right). \tag{3.4}$$

Similarly solving for P_t for downstream lymphangion (assumed to be in diastole) results in

$$P_t = E_{min}\left(\frac{P_{out}}{E_{max}} + SV + V_{o,es} - V_{o,ed}\right). \tag{3.5}$$

To estimate the stroke volume for the first lymphangion, *Eq. 3.4* was set equal to *Eq 5*.

$$SV = \frac{-\left(P_{in} - \alpha E_{max}\left(-V_{o,ed} + V_{o,es}\right) + \alpha\left(P_{out} - E_{max}\cdot V_{o,ed} + E_{max}\cdot V_{o,es}\right)\right)}{\left(1+\alpha\right)^2 \cdot E_{max}} \tag{3.6}$$

Using *Eq. 3.2* and substituting the stroke volume (*Eq. 3.6*), stroke work of the first lymphangion is

$$SW = \frac{-\left(P_{in} - P_{out}\right)\left(P_{in} - \alpha E_{max}\left(-V_{o,ed} + V_{o,es}\right) + \alpha\left(P_{out} - E_{max}\cdot V_{o,ed} + E_{max}\cdot V_{o,es}\right)\right)}{\left(1+\alpha\right)^2 \cdot E_{max}} \tag{3.7}$$

where α is the ratio of E_{min} and E_{max}.

Determination of pressure gradient and stroke work along a series of lymphangions. To illustrate the distribution of pressure along lymphatic vessel operating in two transmural pressure zones, the pressure gradient along a lymphatic vessel consisting of three lymphangions was calculated. First, contraction frequencies and lengths were assumed to be equal. Assuming conservation of mass, lymphangion stroke volumes were also necessarily equal. Furthermore the outlet pressure of an upstream lymphangion was set equal to the inlet pressure for the subsequent lymphangion. The values for E_{max}, E_{min1}, E_{min2}, $V_{o,es}$, $V_{o,ed1}$ and $V_{o,ed2}$ were set to values obtained from the non-linear parameter estimation (Fig. 3.1). In the *low-pressure Zone 1*, where all transmural pressures are below the cutoff pressure (P_c), the inlet pressure was set at 0.25 cmH_2O and stroke volume was set to 0.02 ml. For *the high-pressure Zone 2*, where all transmural pressures are above the cutoff pressure, the inlet pressure was set at 4 cmH_2O and stroke volume was set to 0.175ml. The stroke volume and the inlet pressure were

chosen such that all three lymphangions function in either *Zone 1* or *Zone 2*. The pressure steps and stroke work were calculated using *Eqs. 3.1* and *3.2* for each lymphangion.

3.2 RESULTS

Stroke volume for the two pressure zones. For *Zone 1*, when transmural pressure is less than P_c, (Fig. 3.1), $V_{o,ed}$ and $V_{o,es}$ in *Eq. 3.1* are equal, and the stroke volume for *Zone 1* is thus

$$SV = \left(\frac{P_{in}}{E_{min}} - \frac{P_{out}}{E_{max}} \right). \tag{3.8}$$

For *Zone 2*, when transmural pressure is greater than P_c, (Fig. 3. 1), the end-systolic and end-diastolic pressure-volume relationships have equal slopes, but different intercepts. Substituting the condition, E_{max}=E_{min} in *Eq. 1* yields

$$SV = \left(\frac{P_{in} - P_{out}}{E_{min}} + V_{o,ed} - V_{o,es} \right). \tag{3.9}$$

For *Zone 1*, the stroke volume and stroke work increase with increased transmural pressure (Figs. 3.2C and 3.2E). However in *Zone 2*, there is no change in stroke volume or stroke work with increased transmural pressure (Figs. 3.2D and. 3.2F).

Estimated parameter values. From Figure 3.1, the resulting values for E_{max}, $V_{o,es}$, $V_{o,ed1}$, E_{min2}, P_c, E_{min1}, and $V_{o,ed2}$ were 101.4 cmH_2O/ml, 0.05 ml, 0.05 ml, 101.4 cmH_2O/ml, 2.4 cmH_2O, 11.5 cmH_2O/ml and 0.24 ml, respectively.

Stroke work for lymphangion-lymphangion interaction. For an inlet pressure of 4 cmH_2O and outlet pressure of 5 cmH_2O and assuming symmetrical properties for upstream and downstream lymphangions (i.e., assuming α=1) *SW* is not optimized for the case E_{max}=E_{min} (Fig. 3.3) but instead increases monotonically with α.

Functional homogeneity in a lymphatic vessel. In *Zone 1* where E_{min}<E_{max}, the pressure contribution of each lymphangion increases as transmural pressure increases along the length of the lymphatic vessel (Fig. 3.4A). However, there is equal contribution of pressure from each lymphangion for *Zone 2* (Fig. 3.4C), where E_{min}=E_{max}. Since adjacent lymphangions are set to have equal *SV*, from *Eq. 3.2* they will also contribute equal stroke work (Fig. 3.4D) for *Zone 2*, but have unequal stroke work for *Zone 1* (Fig. 3.4C).

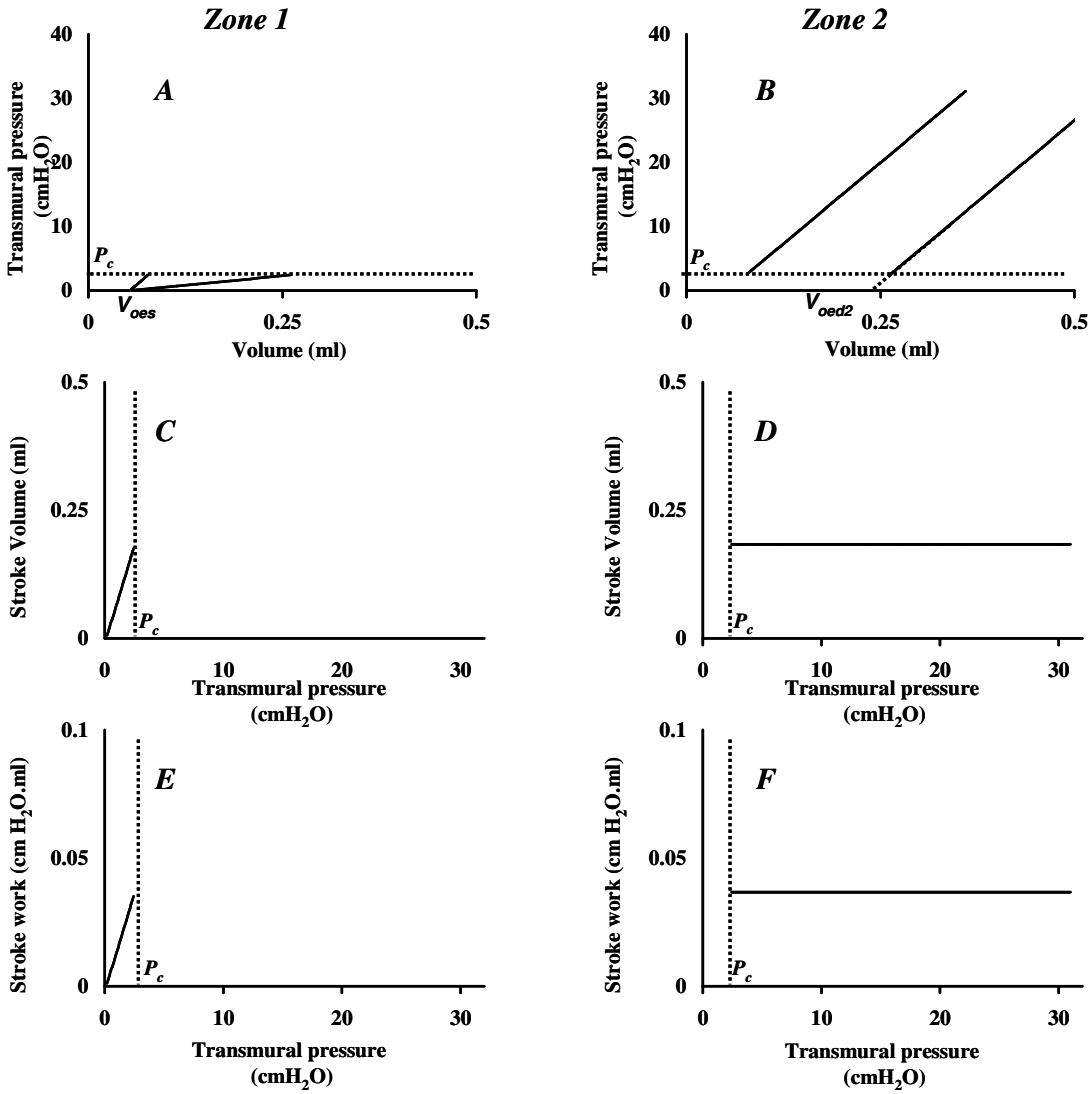

Figure 3.2: Lymphangion pressure-volume relationship for *Zone 1* and *Zone 2* (A and B) based on *Eq. 3.3*. A cutoff pressure (P_c) separates the two zones. Stroke volume (C and E) and stroke work (D and F) were calculated for a lymphangion operating each zone.

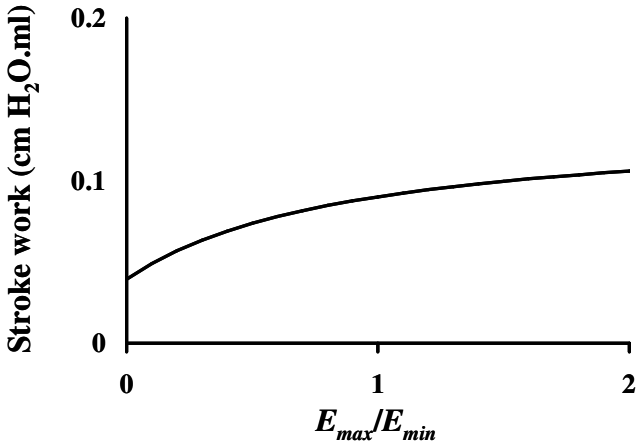

Figure 3.3: Stroke work of the upstream lymphangion is not optimized (maximized) when E_{max} of an upstream lymphangion equals E_{min} of a downstream lymphangion.

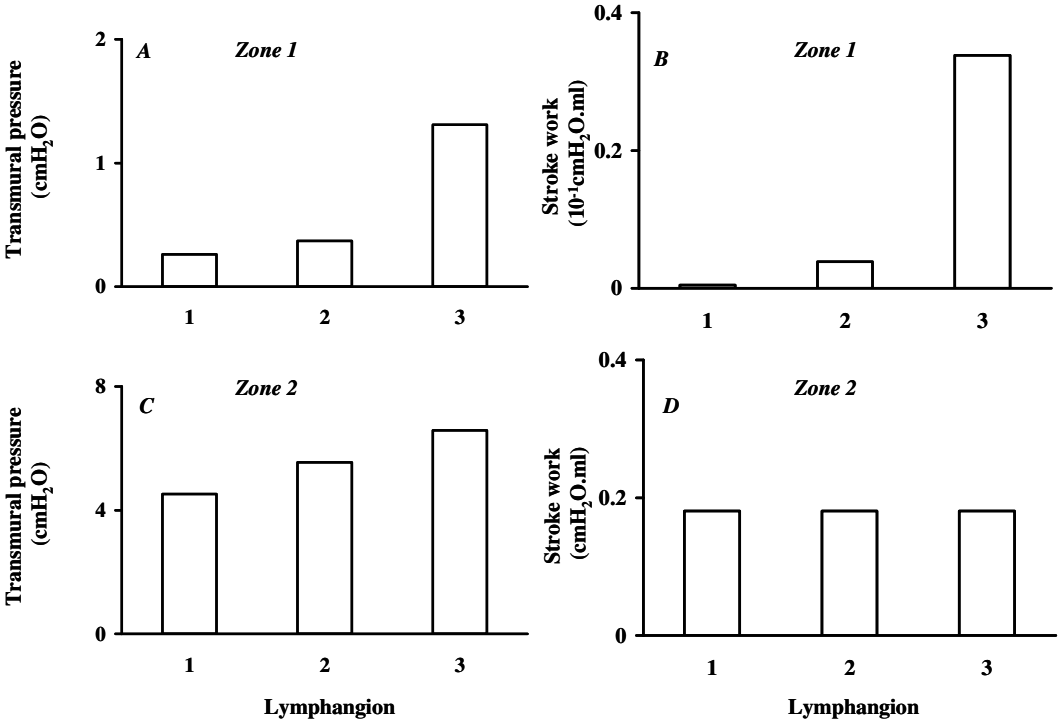

Figure 3.4: Illustration of lymphangion outlet pressure and stroke work for a vessel consisting of 3 lymphangions. (A) For lymphangions in the low-pressure *Zone 1*, the incremental pressure contributed by lymphangions is not equal. (B) Unequal pressure increments in Zone 1 leads to unequal lymphangion stroke work, with stroke work increasing down the length of a lymphatic vessel. (C) Pressure step is equal for all three lymphangions in higher-pressure *Zone 2*. (D) Equal pressure increments lead to equal stroke work in each lymphangion in *Zone 2*.

4. OPTIMAL LYMPHATIC NETWORK

4.1 THEORY

Stroke volume of a lymphangion. In order to predict the stroke volume of a lymphangion analytically (i.e., with an algebraic equation), a simple pressure-volume relationship can be assumed that captures the essence of experimentally-measured values (Fig. 4.1). Taking this approach, Quick et al. (46) developed a simple model to calculate lymphangion stroke volume (*SV*) as a function of the slope of the end-systolic pressure volume relationship (E_{max}), the slope of end-diastolic pressure volume relationship (E_{min}), the inlet pressure (P_{in}), the outlet pressure (P_{out}), and the dead volumes for the end-diastolic and end-systolic pressure-volume relationships ($V_{o,ed}$ and $V_{o,es}$, respectively), represented as V_o in Fig. 4.1.

$$SV = \left(\frac{P_{in}}{E_{min}} - \frac{P_{out}}{E_{max}} + V_{o,ed} - V_{o,es} \right) \tag{4.1}$$

Equation 4.1 is in the functional form first proposed by Sunagawa et al. (52) to characterize ventricular function, and implicitly assumed that the pressure-volume loops are rectangular. The lymphangion model was validated by comparing results with a realistic, complex, detailed lymphangion model (45, 55) and experimental data obtained from post-nodal bovine mesenteric lymphatic vessels (55). By normalizing E_{min} and E_{max} by length (E'_{min} and E'_{max}), lymph flow (Q) from the lymphangion can be expressed as a function of stroke area (SA), length of the lymphangion (l) and frequency (f) of contraction.

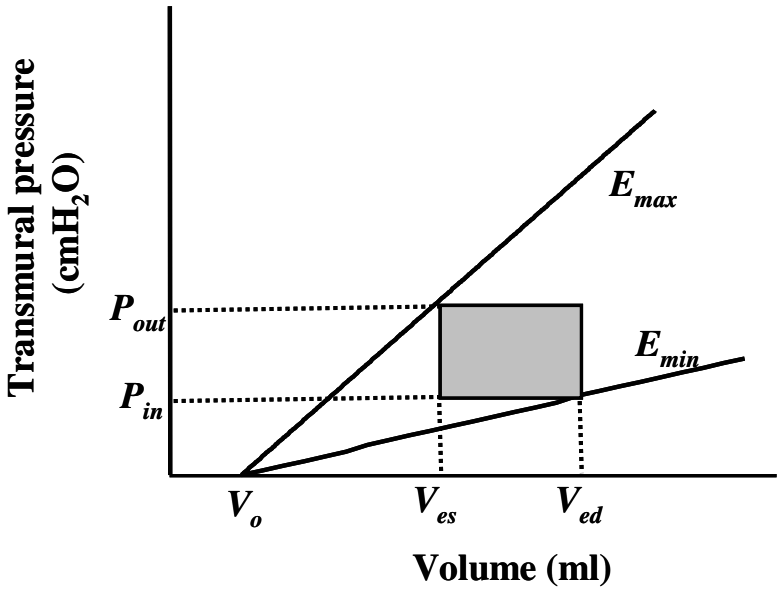

Figure 4.1: Pressure-volume relationship of a lymphatic segment. Stroke volume (V_{ed}-V_{es}) is determined using inlet pressure (P_{in}), outlet pressure (P_{out}), slope of end-systolic pressure volume relationship (E_{max}), slope of end-diastolic pressure volume relationship (E_{min}), and their dead volume (V_o).

$$Q = f \cdot l \cdot SA = f \left[l \cdot \left(\frac{P_{in}}{E'_{min1}} - \frac{P_{out}}{E'_{max1}} \right) + V_{o,ed} - V_{o,es} \right] \quad (4.2)$$

This approximation incorporates the critical assumption that the lymphangion acts as a pump, transporting lymph from a lower pressure to a higher pressure (45).

Lymphangion flow as a function of length. To determine how the length of a lymphangion affects its ability to pump, the pressure gradient it generates (P_L) is assumed constant. The value of P_L characterizes the pressure a lymphangion must generate to transport lymph a particular distance. The inlet and outlet pressure can be expressed as a function of length and transmural pressure.

$$P_{out} = P_{trans} + \frac{l \cdot P_L}{2} \quad (4.3A)$$

$$P_{in} = P_{trans} - \frac{l \cdot P_L}{2} \quad (4.3B)$$

By substituting *Eq*. 4.*3A and 4.3B* in *Eq. 4.2*, flow from the lymphangion can be expressed as a function of length.

$$Q = f \left[\cdot l \cdot \left(\frac{P_{trans} - \frac{l \cdot P_L}{2}}{E'_{min1}} - \frac{P_{trans} + \frac{l \cdot P_L}{2}}{E'_{max1}} \right) + V_{o,ed} - V_{o,es} \right] \quad (4.4)$$

Optimal lymphangion length. Flow from the lymphangion, represented by *Eq. 4.4*, is a parabolic function of length. To obtain the optimal length that produces maximal flow, *Eq. 4.4* is differentiated with respect to length, equated to zero, and was solved for length (l_{opt}).

$$l_{opt} = \frac{P_{trans}}{P_L}\left[\frac{E'_{max} - E'_{min}}{E'_{max} + E'_{min}}\right] \tag{4.5}$$

Lymphangion endothelial shear stress. Endothelial shear stress in a pumping lymphangion is cyclical. The maximum value (τ_{max}) occurs at end-diastole when the radius is largest and the velocity of lymph is the greatest (8). It can be calculated from end-diastolic radius (r_{ed}), lymph viscosity (μ) and flow (Q), given the same assumptions required for Poiseuille's Law (53)

$$\tau_{max} = \frac{4\mu}{\pi r_{ed}^{\,3}} \cdot Q \tag{4.6}$$

Ejection fraction of a lymphangion. Ejection fraction (*EF*), a term commonly used to describe the fraction of blood ejected by the heart in a single contraction, can be applied to lymphangions. The lymphangion *EF* takes a simple form,

$$EF = \frac{A_{ed} - A_{es}}{A_{ed}}, \tag{4.7}$$

where A_{ed} is the calculated area at end of diastole and A_{es} is the area at end of systole.

Structure of lymphangion at a confluence. Assuming conservation of mass, the sum of flow from the two feeding lymphangions (Q_2 and Q_3) equals the flow through the downstream lymphangion (Q_1) (Fig. 4.2).

$$Q_1 = Q_2 + Q_3 \tag{4.8}$$

To keep the nomenclature consistent, the feeding upstream lymphangions are denoted by subscripts 2 and 3 and the downstream lymphangion is represented by a subscript of 1.

Parameters to describe lymphangion at a confluence. Lymphangions at a confluence may not be symmetrical. To characterize the different ratios important for

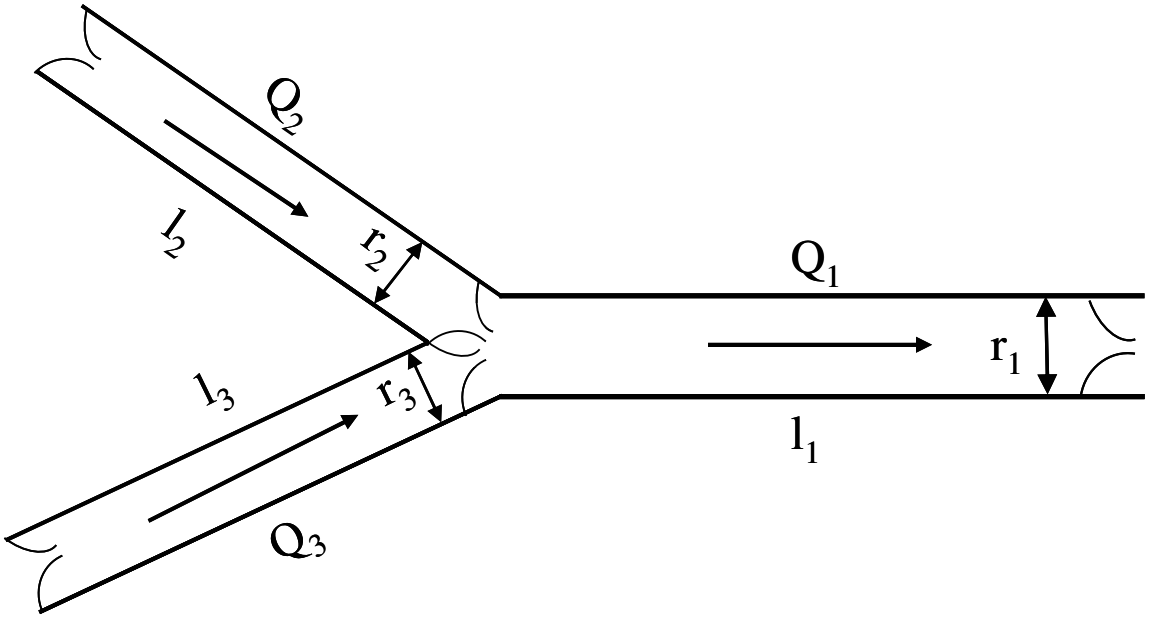

Figure 4.2: Symmetric lymphatic vessel structure at a confluence. Flow is governed by conservation of mass with $Q_1=Q_2+Q_3$. Ratio of lymphangion length (l_1/l_2) and lymphangion radius at end systole (r_1/r_2) is equal to 1.26, assuming a symmetrical network with constant lymphangion endothelial shear stress and ejection fractions.

lymphangion function, three ratios are defined. First, the maximum endothelial shear stress of *lymphangion 1* is a factor α of *lymphangion 2*. Second, flow from *lymphangion 2* is a factor δ of *lymphangion 3*. Third, the ejection fraction of *lymphangion 1* is a factor β of *lymphangion 1*.

$$\alpha = \frac{\tau_{1\,max}}{\tau_{2\,max}} \tag{4.9A}$$

$$\delta = \frac{Q_2}{Q_3} \tag{4.9B}$$

$$\beta = \frac{EF_1}{EF_2} \tag{4.9C}$$

When the lymphatic network is symmetrical, δ is equal to 1. α and β are assumed to be equal to 1, an approximation considering changes of maximal shear and ejection fraction to be negligible at a confluence.

Radius ratio of lymphangions at a confluence. From *Eqs. 4.6, 4. 8* and *4.9*, the ratio of downstream to upstream radii can be expressed as a function of two parameters characterizing the asymmetry in flow and maximum endothelial shear stress

$$\frac{r_{ed1}}{r_{ed2}} = \left(\alpha(\delta+1)\right)^{\frac{1}{3}} \tag{4.10}$$

If the network is assumed to be symmetrical, δ is equal to 1. If the shear stress of the lymphangions at a confluence is equal, α is equal to 1. In this case, the radii of downstream lymphangions are predicted to be larger than that of the feeding upstream lymphangions. From *Eq. 4.10*, the ratio of radii at a confluence that optimizes lymph flow in such a network is equal to 1.26.

Length ratio of the lymphangions at the confluence. Flow (Q) can be calculated as a function of velocity of the lymph (V) and the area of cross section at end diastole (A_{ed}).

$$Q = V \cdot A_{ed} \tag{4.11}$$

The ejection fraction (EF), as given in *Eq. 4.7*, can then be expressed as a function of endothelial shear stress and radius at end-systole by equating flow ($f\ l\ (A_{ed}\text{-}A_{es})$) to *Eq. 4.11* and substituting into *Eq. 4.6*.

$$EF = \frac{\tau_{max} \cdot r_{ed}}{4 \cdot \mu \cdot f \cdot l} \tag{4.12}$$

From *Eqs*. 4.*9* and 4.*12,* the ratio of lengths at a confluence is a function of asymmetry parameter δ and assumed constants α, β, and ϕ, the ratio of downstream to upstream contraction frequencies (f_1/f_2).

$$\frac{l_1}{l_2} = \varphi \cdot \frac{\alpha \cdot \beta}{(\alpha(\delta+1))^{\frac{1}{3}}}, \tag{4.13}$$

If the network is assumed to be symmetrical, and all lymphangion frequencies, shear stress and ejection fraction are assumed to be equal (i.e., α, δ and ϕ are equal to 1), the lengths of downstream lymphangions are predicted to be longer than the upstream lymphangions. From *Eq. 4.13*, the ratio of lengths at a confluence in such a network is equal to 1.26.

4.2 METHODS

Optimal lymphangion length. Equation 4 was used to identify the optimal length for maximal flow at transmural pressures (P_t) of 0.1 and 2.4 cmH_2O for a P_L of 0.5 cmH_2O/cm.. Consistent with values used in lymphangion models reported by Venugopal et al. (Section 3). Values for E_{min} and E_{max}, obtained from post-nodal bovine mesenteric lymphatic vessels, were set at 11.5 cmH_2O/ml and 101.4 cmH_2O/ml, respectively, and $V_{o,ed}$ and $V_{o,es}$ was set to 0.05 ml. The values of P_t, E_{min} and V_o, (Fig. 4.1) correspond to the low-pressure zone characterized previously (Section 3). Flow from the lymphangion was calculated for a frequency of 5 contractions per minute.

Theoretical radius change along the network of lymphatic vessels. To identify the number of confluences in a lymphatic network optimized for flow, lymphangion radius was plotted as a function of the confluence number. To simplify, it was assumed that the ratios α and δ were equal to 1. The range of radii assumed was from 3 mm to 30 μm (thoracic duct of a human to a microvessel). The number of confluence (n) was then predicted using *Eq. 4.10* by scaling the lymphangion radius by a factor of 1.26.

Length changes along the network of lymphatic vessels. To identify how the lymphangion length scales from the thoracic duct to the microvessels in a lymphatic network optimized for lymph flow, we assumed that the ratios α, β, δ, and ϕ are equal to 1. Thoracic duct radius was assumed to be 3 mm. Lengths were calculated from *Eq. 4.13* for the number of confluences in the network (n) and plotted. The length of a terminal lymphangion was predicted assuming thoracic duct length and n.

Measured lengths of lymphangions. Post-nodal bovine mesenteric lymphatic vessels were obtained from an abattoir in order to test the theoretical predictions of *Eq. 4.13*. Lymphatic vessels were identified by injecting an Evan's blue dye-based saline solution into the lymph nodes. After locating a lymphatic vessel, the lymphangions were identified by identifying the valves The distance between the valves for the lymphangions (Fig. 4.2) was measured using a digital caliper.

4.3 RESULTS

Optimal lymphangion length. The mathematical model (*Eq. 4.4*) indicates that lymphangions exhibit an optimal length that produces maximal flow . The optimum is predicted to occur at a length of 0.2 cm and 5.1 cm for post-nodal bovine mesenteric lymphangions at transmural pressures of 0.1 cmH_2O and 2.4 cmH_2O respectively (Fig. 4.3). The optimum can vary considerably depending on P_L used in *Eq. 4.4*, with a 9.4 % change in the optimum for 10% change in its value. However, for given set of parameters, a 10% change in length results in a flow reduction of only 1%, suggesting near optimal structure for lymphangion. The predicted optimal lengths for the low pressure transmural pressures have a range that includes the experimentally measured length of 1.14 + 0.5 cm (Fig. 4.3).

Predicting the number of bifurcations from microvessels to conducting vessels. The number of confluences required for an optimal network of lymphangions with radii ranging from 3 mm to 30 μm is 21 (Fig. 4.4A).

Predicting the length of a terminal lymphangion for a given thoracic duct length. Using thoracic duct length from previously reported studies (5), we found that for 21 confluences in a lymphatic network, the lymphangion length of a vessel with radius of 30 μm is 294 μm (Fig. 4.4B).

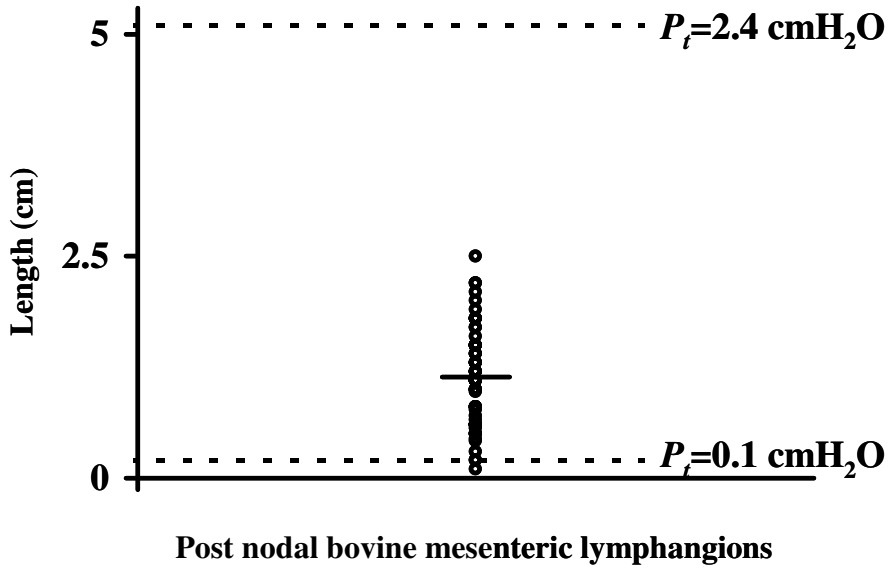

Figure 4.3: Length (open circles) values (74) obtained from post-nodal bovine mesenteric lymphatic vessel with a mean of 1.14 cm (solid line). Equation *4.5* was used to predict the optimal length predictions for transmural pressure of 0.1 cmH_2O and 2.4 cm H_2O (dotted lines).

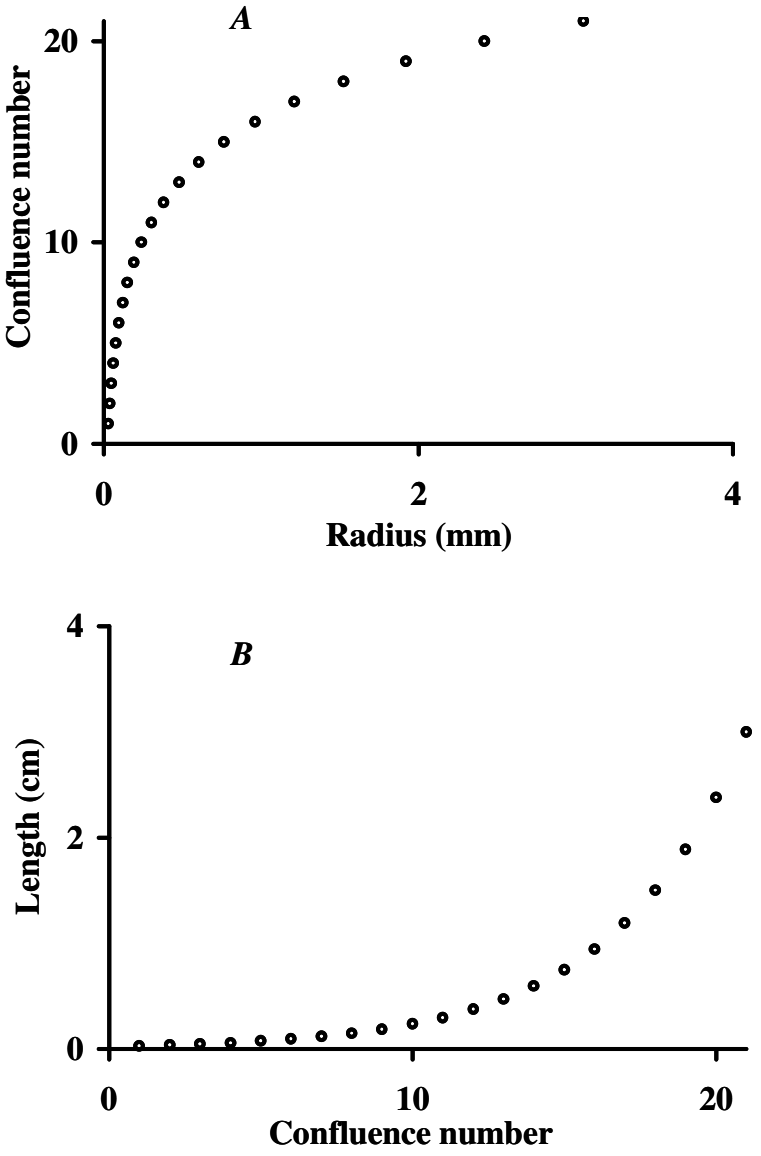

Figure 4.4: Relationship between lymphangion length, radius and the confluence number. A) Radius of lymphangion, identified for a microvessel and a thoracic duct is used to predict the number of confluences between them as 26. B) For 26 confluences, the length of the lymphangion scales from 3 cm in thoracic duct to 294 μm in an initial lymphatic of radius 30 μm.

5. DISCUSSION AND CONCLUSIONS

5.1 ACTIVE DIAMETER RESPONSE TO CHANGES IN LYMPHATIC PRESSURE

Our data demonstrate that bovine mesenteric lymphatic segments responded to a step increase in transmural pressure with an active decrease in end-diastolic diameter — a myogenic response, comparable to that reported in arterioles and venules (6, 7). A complementary increase in end-diastolic diameter was observed in response to a pressure decrease. The magnitude of this myogenic response was proportional to the pressure step that induced it and was sufficient to result in a negative relationship between end-diastolic diameter and transmural pressure. The lymphatic myogenic response required approximately four minutes to reach a new steady state end-diastolic diameter. This is similar to the venular response, but notably longer than the myogenic response of arterioles which is complete within 10-15 seconds (6, 7).

Lymphatic vessels share structural and functional similarities with veins and venules. They have relatively thin walls and unidirectional valves. Some venules and veins display intrinsic phasic contractile behavior (7, 29). Furthermore, both lymphatic vessels and venules exhibit a rate-sensitivity to changes in pressure (7). The lymphatic myogenic response is similar to that reported by Davis et al. in an *in vitro* study of bat wing venules(7). However, unlike the present study of lymphatic vessels, contraction frequency in venules increased significantly in response to a step increase in transmural pressure. In a similar study of skeletal muscle venules, Johansson and Mellander (29)

demonstrated that venular diameter decreases with an increase in pressure and increases with a decrease in pressure.

Hargens et al. used the term “myogenic” to describe the intrinsic origin of the phasic contractile behavior of lymphatic vessels(27). Later, the term “myogenic response” was used to describe the observations by Mizuno et al. and Hosaka et al. in rat iliac lymphatic vessels (diameters 250 μm) that steady-state end-diastolic diameters did not change significantly in response to changes in transmural pressure from 3 to 9 cmH_2O (28, 40). The present study, however, demonstrated that steady-state end-diastolic diameters of bovine mesenteric lymphatic vessels significantly decreased in response to increases in transmural pressure, much like muscular arterioles. Differences between the findings of those earlier studies and the current findings may be the result of differences in 1) vessel sizes 2) the tissues from which the vessels were collected, 3) the data analysis methods or 4) the magnitude of luminal flow or shear stress.

The active tension generated by lymphatic vessels has been shown to change in response to changes in vessel diameter (59). Because circumferential wall tension is the product of pressure and vessel radius, microlymphatic vessels (diameter 150 μm) have a lower tension than bovine mesenteric vessels (2-6 mm) for the same transmural pressure. For the same reason, a step change in pressure results in a greater change in wall tension in large compared to small vessels. Thus, if the lymphatic myogenic response is modulated by a change in tension rather than pressure, the response might be a more pronounced phenomenon in large vessels.

Lymphatic vessels in different regions of the lymphatic network exhibit functional differences. Gashev et al. evaluated the lymphatic contractility of rat thoracic duct, mesenteric, cervical, and femoral lymphatics, and found that mesenteric vessels are stronger pumps than the thoracic duct (22). Similarly, the strength and sensitivity of the lymphatic myogenic response may vary with region.

By using regression analysis, we have been able to show that that lymphatic end-diastolic diameter decreases in response to an increase in transmural pressure. The previous reports of the lymphatic myogenic response used analysis of variance, a method that is less sensitive to proportional relationship between the independent and dependent variables (25).

In vitro lymphatic studies have classically used isobaric preparations with flow through the lymphatic vessel to characterize pressure responses (17, 35). Recent studies by Gashev et al. demonstrated that increased flow (and presumably endothelial shear stress) caused dilation of lymphatic vessels and a decrease in contraction frequency (23). This shear-mediated response confounds the results obtained from previous studies purporting to report only pressure-mediated responses. More recently, Gasheva et al. (24) reported that lymphatic vessel contraction generates significant shear stress, causing the endothelial cells to release nitric oxide to relax lymphatic smooth muscle. To minimize these shear mediated effects, we used an isobaric preparation without flow though the vessel lumen. Shear effects may diminish the lymphatic myogenic effect in a flow-through preparation.

The lymphatic myogenic response observed in this study occurred following a change in transmural pressure in the presence of low flow and, thus, may best represent an aspect of lymphatic function during downstream lymphatic obstruction. Lymphatic vessels display a length-tension relationship characterized by development of peak tension at an optimal length (38). By actively regulating the end-diastolic diameter, the myogenic response may allow lymphatic vessels to continue to operate near their optimal length despite changes in transmural pressure.

5.2 OPTIMAL LYMPHATIC END-DIASTOLIC ELASTANCE

Stroke volume and stroke work are filling-independent above a cutoff pressure. The present work reveals that when the slope of the end-systolic pressure-volume relationship (E_{min}) and the end-diastolic pressure-volume relationship (E_{max}) are equal, both stroke volume and stroke work is insensitive to transmural pressure (Fig. 3.2). The analogy of the ventricle that cardiac stroke work is optimized when E_{max} of the pump (heart) equals E_{min} of the downstream segment (arterial system) was used to analyze previously published pressure-volume relationships of the lymphangion. We found that, indeed, above a cutoff pressure, the value of E_{min} is approximately equal to E_{max} (Fig. 3.1). However, stroke work is not optimized when E_{max} of the upstream lymphangions is equal to E_{min} of the downstream lymphangion (Fig. 3.3). Whereas most investigators describe the end-diastolic pressure-volume relationship with an empirical exponential function to fit the data (34, 43), we analyze the pressure-volume relationship into two distinct zones (*Eq. 3.1*) that yield different behaviors. Below a cutoff pressure,

lymphangion stroke volume and stroke work increase with filling pressure, analogous to the Frank-Starling mechanism (Figs. 3.2C and E). Above the cutoff pressure, lymphangion stroke volume is independent of pressure, analogous to blood flow autoregulation (6) (Figs. 3.2D and F). Lymphangions in series also produce equal pressure steps (Fig. 3.4B), which has been observed experimentally (16). Equal pressure steps also ensure equal stroke work for all the lymphangions in the lymphatic vessel when they have the same stroke volumes. In addition to these two pressure zones, there is a third zone (typically >32 cmH_2O) where stroke volume decreases with pressure (32). Thus, a segmented linear end-diastolic diameter can explain a number of previously observed phenomenon in lymphatic vessels.

Accommodating two anti-edema mechanisms: transition from preload-dependent stroke volume to afterload-independent stroke volume. Interstitial fluid volume is regulated by the interaction of microvascular filtration, interstitial compliance, and lymphatic flow (1). Whenever one property cannot adequately adapt to changes in the other two, fluid can accumulate, resulting in interstitial edema (9). Although in vitro experiments have elucidated that transmural pressure has a significant effect on lymphatic pumping (18, 37), considerably less is known about how different edemagenic conditions alter lymphatic transmural pressures in vivo (20, 21). Because interstitial compliance can increase with volume (1), however, significant increases in microvascular pressure can typically increase microvascular filtration and thus lymphatic transmural pressure by only 5 cmH_2O (4). On the other hand, increases in lymphatic outlet pressure due to venous hypertension can raise lymphatic outlet pressure (and thus

lymphatic transmural pressure) as much as 25 cmH_2O (12, 14). These two edemagenic conditions imply a need for lymphangions to have different responses in two pressure ranges. In the first low-pressure condition, lymphangions need to pump greater volumes of lymph to accommodate higher transvascular fluxes (4). In the second high-pressure condition, lymphangions do not have to pump more, but instead must maintain a constant flow as reported previously (14). The predicted transition from preload-dependent stroke volume to afterload-independent stroke volume thus accommodates the disparate requirements for two different anti-edema mechanisms.

Pump capacity depends on either the slopes or the intercepts of lymphangion pressure–volume relationships. The simple analytical formula for lymphangion stroke volume (*Eq. 3.1*) provides unique insight to explore the relative importance of lymphangion structural properties. Because lymphangion properties are different above and below a cutoff pressure (Fig. 3.2), the sensitivity to changes in the parameters is strikingly different. To illustrate, a simple "parameter sensitivity analysis" was performed to determine how much stroke volume would change for a 10% change in parameters. Below the cutoff pressure (i.e., *Zone 1*), the dead volume (i.e. the intercept of the end-diastolic pressure-diameter relationship) does not have any effect on stroke volume. Above the cutoff pressure (i.e., *Zone 2*), however, a 10% increase in either the end-diastolic ($V_{o,ed}$) or end-systolic ($V_{o,es}$) dead volumes results in a change of more than 100% in stroke volume. Combining these parameters, the differential dead volume ($\Delta V_o = V_{o,ed}\text{-}V_{o,es}$) arises as an independent variable in *Eq. 3.1*. The sensitivity of stroke work to ΔV_o (45%) is similar to the sensitivities to E_{min} (53%) or E_{max} (45%). Although E_{min}

has been used as an index of lymphangion diastolic tone (15), and E_{max} has been used as an index of systolic contractility (34, 45), ΔV_o emerges as an independent, novel index of pump function.

Demarcation of two zones. Transmural pressure is used as an index to delineate the two zones of pressure volume relationship. The cutoff pressure (P_c), E_{min} for *Zone 1* and dead volume for *Zone 2* ($V_{oed,2}$) were identified using nonlinear parameter estimation, a method that allows more that one variable to have values with least error, compared to the data. We also assumed that E_{max} and E_{min} for *Zone 2* are equal. The parameter values obtained by different assumptions and analysis will predict different values. For example, in addition to assuming E_{min2}, we could also assume a cutoff pressure at 7 cmH_2O, and calculate the corresponding E_{min1}. This means we make P_c a constant along with the E_{min} of *Zone 2*, allowing only E_{min} of *Zone 1* and dead volume to change. However, using this approach would introduce significant error to our estimate of E_{min1}. This work thus shows that there are two zones of pressure-volume relationship for the lymphangions and that the values used to demarcate the zone can be different. This approach is inductive, where an assumption is made to predict the result, and not deductive like most experimental approaches.

Simple approximations allow prediction of global behavior. The present work extended a previously-reported lymphangion model (46) that was thoroughly validated by comparing its predictions to experimental data on the one hand, and a detailed numerical model (55) on the other. This model neglects lymph inertia and viscosity, since they have negligible effects on developed pressure gradients when the

lymphangion acts as a pump. However, this assumption makes the model inappropriate to characterize conduit behavior that arises when the normal axial pressure gradient reverses (45). More importantly, the present model does not include the effects of endothelial shear stress, which is known to cause dilation at high flows and even pump inhibition (23). The assumption of a constant time-varying elastance implicitly assumes that baseline lymphangion contractility and tone do not change with flow. To use the present model to predict lymph flow over very wide ranges, it would be necessary to adjust the tone and contractility (E_{min}, E_{max}) and the dead volumes ($V_{o,es}$, $V_{o,ed}$) appropriately. The most important simplification of this model is the effect of contraction frequency, which increases with transmural pressure (37). To derive stroke work, it was assumed that contraction frequency does not change. Adding this complication, however, would improve the model's ability to describe observed pressure-volume relationships.

Theoretical analysis explains observed behavior. By using cardiac analogies and assuming that the slopes of ESPVR and EDPVR are equal has provided some key insights for basic questions such as why the end-diastolic pressure-volume relationship in a lymphangion is highly nonlinear (34), how lymphangions are able to maintain flows with changes in outlet pressure (14), and why lymphangions in series maintain equal pressure increments despite increases in transmural pressures (16). Importantly, we have identified a mechanism by which the lymphatic system is able to maintain flow during extreme boundary conditions to support continued protein turnover, immune function and lipid absorption. None of these insights can arise from experimental approaches, but

instead from mathematical modeling based on measured lymphangions properties and fundamental physical principles.

5.3 A FRACTAL LYMPHATIC NETWORK STRUCTURE

Based on fundamental principles, this work provides a theoretical determination of a lymphatic system structure that optimizes lymph flow. First, lymphatic vessels will provide the greatest flow when the lymphangions have a particular length. Second, the downstream vessel at a confluence has a length and radius which is a simple factor larger than the two feeding upstream vessels in a lymphatic network, predicting that the lymphangions are progressively longer and bigger from initial lymphatics to thoracic duct. The resulting lymphatic network structure is best described as a fractal, since the geometry is preserved independent of its scale (19). Predictions of lengths are consistent with data we collected from bovine mesenteric lymphatic vessels. The analytical solutions describing lymphangion flow has allowed the use of structural parameter as a variable, allowing a rare deductive approach to deriving fundamental teleological principles.

Two zones of pressure-volume relationship in a lymphangion. The pressure-volume relationship of a lymphangion exhibits two disparate zones (Section 3). In the first, low-pressure zone, lymphangion stroke volume increases with increases in transmural pressure. In this zone, $E_{min}<E_{max}$, and the intercepts of the end-diastolic and end-systolic pressure-volume relationships are nearly equal. This sensitivity to transmural pressure allows feedback to ensure that increases in transvascular flux and

ensuing increases in interstitial pressure will be countered with increased lymphatic pumping. Above a cutoff pressure lies a second high-pressure zone, where $E_{min} \sim E_{max}$ and the there are two distinct intercepts for the end-diastolic and end-systolic pressure-volume relationships (Section 3). As a result, stroke volume and stroke work become insensitive to transmural pressures. It was speculated that in this second zone lymphangions are able to maintain flow over wide ranges of high transmural pressures that can arise from increased outlet pressures (21). Since it is likely that lymphangions are normally subjected to very low pressures, the present work characterized an optimal lymphatic network structure for the low pressure zone, basing all model parameters used for simulation on the low-pressure range of the pressure-volume relationships of bovine mesenteric post-nodal vessels.

Optimal length of a lymphangion. This work predicts that there is an optimal length of a lymphangion that provides maximal flow. This optimal length is however dependant on the transmural pressure of the lymphangion. The range of transmural pressures were determined by the cutoff pressure defined for the pressure-volume relationship described previously. The predicted lymphangion lengths of 0.2 cm and 5.1 cm include the lymphangion length measured from bovine mesenteric lymphangions. The closeness of the prediction may be misleading, since an optimal length depends on a number of parameters (*Eq. 4.5*) such as lymphangion's contractility (E_{max}), tone (E_{min}), contraction frequency (f) and pressure gradient (P_L). However, the predicted change in optimal length resulting from a 10% change in the values of P_L, E'_{min}, E'_{max} is less than 9.4 %. The observed optimum results from two competing factors. First, as length

increases, the stroke volume increases proportionally. Second, as the length increases above the optimum value, the pressure contributed by the lymphatic smooth muscle fails to overcome the axial pressure gradient against which the lymph has to be transported limiting flow. The existence of an optimum suggests two physiological principles. First, once established, length cannot adapt as readily as lymphangion frequency, contractility or tone. Thus, it is critical to have a lymphangion length with the ability to adapt to acute changes in axial pressure gradients. Second, the present work suggests that there is a yet undiscovered developmental mechanism that places valves in the appropriate place.

Optimal network structure. To characterize the structure of a lymphatic network, it is not only necessary to specify the lengths of lymphangions, but also the ratios of lymphangion radii and lengths at confluences. In the present work, we utilized assumption of constant endothelial shear stress to determine the ratio of radii. Calculating endothelial shear stress from the flow data reported for bovine mesenteric lymphangions (45) and rat mesentery lymphangions (8) results in shear stress ranges from 3-12 dynes/cm^2. This range is even smaller than that for the arterial system (44) for which Murray's Law was originally developed.

Validity of basic assumed network properties. Four fundamental assumptions are made to arrive at the final set of equations characterizing optimal lymphatic system structure (*Eqs. 4.5, 4.10* and *4.13*). 1) The maximum shear stress was calculated using the radius at end-diastole. Lymph velocity is not always highest when radius is largest, and peak shear does not always occur at end diastole (8). Although this approximation likely overestimates the value of peak endothelial shear stress, it may not have a large

effect on the ratio of radii. 2) Lymphangion endothelial shear stresses, contraction frequencies and ejection fractions at confluences are assumed to be constant. Although each vary from terminal lymphatic vessels to thoracic ducts, the amount that each vary at a confluence (given the approximately 21 confluences) is exceedingly small. 3) The analytical approximation used to derive an optimal lymphangion length of the lymphangion assumed lymphangions were acting as pumps. This approximation fails when the inlet pressure rises above outlet pressures (33, 41), causing lymphangions to act like conduits (45). 4) The lymphangions at a confluence were assumed to be symmetrical. Although a change in this assumption can change the predicted ratio of 1.26, the predicted result that the downstream lymphangions are longer and bigger than the upstream lymphangion would not be altered. Although these assumptions could be made more realistic, the cost to conceptual clarity may be too high, since analytical solutions are necessary to mathematically derive an optimum.

REFERENCES

1. **Aukland K, Reed RK.** Interstitial-lymphatic mechanisms in the control of extracellular fluid volume. *Physiol Rev* 73: 1-78, 1993.
2. **Bayliss WM.** On the local reactions of the arterial wall to changes of internal pressure. *J Physiol* 28: 220-231, 1902.
3. **Beightler CS, Phillips DT, Wilde DJ.** *Foundations of Optimization*. Englewood Cliffs, New Jersey: Prentice-Hall, 1979.
4. **Benoit JN, Zawieja DC, Goodman AH, Granger HJ.** Characterization of intact mesenteric lymphatic pump and its responsiveness to acute edemagenic stress. *Am J Physiol Heart Circ Physiol* 257: H2059-2069, 1989.
5. **Borisov AV.** The theory of the design of the lymphangion. *Morfologiia* 112: 7-17, 1997.
6. **Davis MJ, Hill MA.** Signaling mechanisms underlying the vascular myogenic response. *Physiol Rev* 79: 387-423, 1999.
7. **Davis MJ, Shi X, Sikes PJ.** Modulation of bat wing venule contraction by transmural pressure changes. *Am J Physiol Heart Circ Physiol* 262: H625-634, 1992.
8. **Dixon JB, Greiner ST, Gashev AA, Cote GL, Moore JE, Zawieja DC.** Lymph flow, shear stress, and lymphocyte velocity in rat mesenteric prenodal lymphatics. *Microcirculation* 13: 597-610, 2006.
9. **Dongaonkar RM, Quick CM, Stewart RH, Drake RE, Cox Jr CS, Laine GA.** Edemagenic gain and interstitial fluid volume regulation. *Am J Physiol Regul Integr Comp Physiol*, 2007.
10. **Drake R, Giesler M, Laine G, Gabel J, Hansen T.** Effect of outflow pressure on lung lymph flow in unanesthetized sheep. *J Appl Physiol* 58: 70-76, 1985.
11. **Drake RE, Abbott RD.** Effect of increased neck vein pressure on intestinal lymphatic pressure in awake sheep. *Am J Physiol* 262: R892-894, 1992.
12. **Drake RE, Abbott RD.** Effect of increased neck vein pressure on intestinal lymphatic pressure in awake sheep. *Am J Physiol Integr Comp Physiol* 262: R892-894, 1992.
13. **Drake RE, Allen SJ, Katz J, Gabel JC, Laine GA.** Equivalent circuit technique for lymph flow studies. *Am J Physiol* 251: H1090-1094, 1986.
14. **Drake RE, Gabel JC.** Effect of outflow pressure on liver lymph flow in unanesthetized sheep. *Am J Physiol Integr Comp Physiol* 259: R780-785, 1990.
15. **Drake RE, Weiss D, Gabel JC.** Active lymphatic pumping and sheep lung lymph flow. *J Appl Physiol* 71: 99-103, 1991.
16. **Eisenhoffer J, Kagal A, Klein T, Johnston MG.** Importance of valves and lymphangion contractions in determining pressure gradients in isolated lymphatics exposed to elevations in outflow pressure. *Microvasc Res* 49: 97-110, 1995.
17. **Elias RM, Johnston MG.** Modulation of fluid pumping in isolated bovine mesenteric lymphatics by a thromboxane/endoperoxide analogue. *Prostaglandins* 36: 97-106, 1988.

18. **Elias RM, Wandolo G, Ranadive NS, Eisenhoffer J, Johnston MG.** Lymphatic pumping in response to changes in transmural pressure is modulated by erythrolysate/hemoglobin. *Circ Res* 67: 1097-1106, 1990.
19. **Falconer KJ.** *Fractal Geometry : mathematical foundations and applications*. Chichester, England: Wiley, 2003.
20. **Gabel JC, Dhother S, Drake RE.** Increased abdominal lymph flow increases lung lymphatic outflow pressure in sheep. *Lymphology* 27: 189-192, 1994.
21. **Gabel JC, Dhother S, Drake RE.** Increased lymphatic pressure without increased neck vein pressure during intravenous infusions. *Am J Physiol* 266: R1596-1598, 1994.
22. **Gashev AA, Davis MJ, Delp MD, Zawieja DC.** Regional variations of contractile activity in isolated rat lymphatics. *Microcirculation* 11: 477-492, 2004.
23. **Gashev AA, Davis MJ, Zawieja DC.** Inhibition of the active lymph pump by flow in rat mesenteric lymphatics and thoracic duct. *J Physiol* 540: 1023-1037, 2002.
24. **Gasheva OY, Zawieja DC, Gashev AA.** Contraction-initiated NO-dependent lymphatic relaxation: a self-regulatory mechanism in rat thoracic duct. *J Physiol* 575: 821-832, 2006.
25. **Glantz SA.** *Primer of Biostatistics*. New York: McGraw-Hill, 1992.
26. **Glenny RW, Robertson HT, Yamashiro S, Bassingthwaighte JB.** Applications of fractal analysis to physiology. *J Appl Physiol* 70: 2351-2367, 1991.
27. **Hargens AR, Zweifach BW.** Contractile stimuli in collecting lymph vessels. *Am J Physiol Heart Circ Physiol* 233: H57-65, 1977.
28. **Hosaka K, Mizuno R, Ohhashi T.** Rho-Rho kinase pathway is involved in the regulation of myogenic tone and pump activity in isolated lymph vessels. *Am J Physiol Heart Circ Physiol* 284: H2015-2025, 2003.
29. **Johansson B, Mellander S.** Static and dynamic components in the vascular myogenic response to passive changes in length as revealed by electrical and mechanical recordings from the rat portal vein. *Circ Res* 36: 76-83, 1975.
30. **Kamiya A, Bukhari R, Togawa T.** Adaptive regulation of wall shear stress optimizing vascular tree function. *Bull Math Biol* 46: 127-137, 1984.
31. **Kuo L, Davis MJ, Chilian WM.** Endothelium-dependent, flow-induced dilation of isolated coronary arterioles. *Am J Physiol Heart Circ Physiol* 259: H1063-1070, 1990.
32. **Laine GA, Allen SJ, Katz J, Gabel JC, Drake RE.** Outflow pressure reduces lymph flow rate from various tissues. *Microvasc Res* 33: 135-142, 1987.
33. **Laine GA, Hall JT, Laine SH, Granger J.** Transsinusoidal fluid dynamics in canine liver during venous hypertension. *Circ Res* 45: 317-323, 1979.
34. **Li B, Silver I, Szalai JP, Johnston MG.** Pressure-volume relationships in sheep mesenteric lymphatic vessels in situ: response to hypovolemia. *Microvasc Res* 56: 127-138, 1998.
35. **McHale NG, Allen JM.** The effect of external Ca2+ concentration on the contractility of bovine mesenteric lymphatics. *Microvasc Res* 26: 182-192, 1983.
36. **McHale NG, Meharg MK.** Co-ordination of pumping in isolated bovine lymphatic vessels. *J Physiol* 450: 503-512, 1992.

37. **McHale NG, Roddie IC.** The effect of transmural pressure on pumping activity in isolated bovine lymphatic vessels. *J Physiol* 261: 255-269, 1976.
38. **Meisner JK, Stewart RH, Laine GA, Quick CM.** Lymphatic vessels transition to state of summation above a critical contraction frequency. *Am J Physiol Regul Integr Comp Physiol* 293: R200-208, 2007.
39. **Mislin H.** Active contractility of the lymphangion and coordination of lymphangion chains. *Experientia* 32: 820-822, 1976.
40. **Mizuno R, Dornyei G, Koller A, Kaley G.** Myogenic responses of isolated lymphatics: modulation by endothelium. *Microcirculation* 4: 413-420, 1997.
41. **Mortillaro NA, Taylor AE.** Interstitial fluid pressure of ileum measured from chronically implanted polyethylene capsules. *Am J Physiol* 257: H62-69, 1989.
42. **Murray CD.** The Physiological Principle of Minimum Work: I. The Vascular System and the Cost of Blood Volume. *Proc Natl Acad Sci U S A* 12: 207-214, 1926.
43. **Ohhashi T, Azuma T, Sakaguchi M.** Active and passive mechanical characteristics of bovine mesenteric lymphatics. *Am J Physiol Am J Physiol Heart Circ Physiol* 239: H88-95, 1980.
44. **Pries AR, Secomb TW, Gaehtgens P.** Design principles of vascular beds. *Circ Res* 77: 1017-1023, 1995.
45. **Quick CM, Venugopal AM, Gashev AA, Zawieja DC, Stewart RH.** Intrinsic pump-conduit behavior of lymphangions. *Am J Physiol Regul Integr Comp Physiol* 292: R1510-1518, 2007.
46. **Quick CM, Venugopal AM, Laine GA, Stewart RH.** First-order approximation for the lymphangion pressure-flow relationship. *Am J Physiol Heart Circ Physiol* (in press).
47. **Reddy NP, Krouskop TA, Newell PH, Jr.** Biomechanics of a lymphatic vessel. *Blood Vessels* 12: 261-278, 1975.
48. **Reddy NP, Krouskop TA, Newell PH, Jr.** A computer model of the lymphatic system. *Comput Biol Med* 7: 181-197, 1977.
49. **Rossitti S, Lofgren J.** Vascular dimensions of the cerebral arteries follow the principle of minimum work. *Stroke* 24: 371-377, 1993.
50. **Suga H, Sagawa K.** Instantaneous pressure-volume relationships and their ratio in the excised, supported canine left ventricle. *Circ Res* 35: 117-126, 1974.
51. **Suga H, Sagawa K, Shoukas AA.** Load independence of the instantaneous pressure-volume ratio of the canine left ventricle and effects of epinephrine and heart rate on the ratio. *Circ Res* 32: 314-322, 1973.
52. **Sunagawa K, Sagawa K, Maughan WL.** Ventricular interaction with the loading system. *Ann Biomed Eng* 12: 163-189, 1984.
53. **Sutera SP, Skalak R.** The History of Poiseuille's Law *Annual Review of Fluid Mechanics* 25: 1-20, 1993.
54. **Taber LA, Ng S, Quesnel AM, Whatman J, Carmen CJ.** Investigating Murray's law in the chick embryo. *J Biomech* 34: 121-124, 2001.
55. **Venugopal AM, Stewart RH, Laine GA, Dongaonkar RM, Quick CM.** Lymphangion coordination minimally affects mean flow in lymphatic vessels. *Am J Physiol Heart Circ Physiol* 293: H1183-1189, 2007.

56. **Venugopal AM, Stewart RH, Rajagopalan S, Laine GA, Quick CM.** Optimal lymphatic vessel structure. *Conf Proc IEEE Eng Med Biol Soc* 5: 3700-3703, 2004.
57. **von der Weid PY, Zawieja DC.** Lymphatic smooth muscle: the motor unit of lymph drainage. *Int J Biochem Cell Biol* 36: 1147-1153, 2004.
58. **Zawieja DC, Davis KL, Schuster R, Hinds WM, Granger HJ.** Distribution, propagation, and coordination of contractile activity in lymphatics. *Am J Physiol Heart Circ Physiol* 264: H1283-1291, 1993.
59. **Zhang RZ, Gashev AA, Zawieja DC, Davis MJ.** Length-tension relationships of small arteries, veins, and lymphatics from the rat mesenteric microcirculation. *Am J Physiol Heart Circ Physiol* 292: H1943-1952, 2007.

VITA

Name:	Arun Madabushi Venugopal
Address:	Hwy 60, VMA, Room 300A, VTPP, Texas A&M University, College Station, Texas-77843-4466
Email Address:	arunmv@gmail.com
Education:	B.E., Instrumentation and Control Engineering, University of Madras, 2002.
	M.S., Biomedical Engineering, Texas A&M University, 2004.
	Ph.D., Biomedical Sciences, Texas A&M University, 2008.